doi:10.1093/brain/awz320 BRAIN 2019: 0; 1–15 | 1

BRAIN
A JOURNAL OF NEUROLOGY

Hypersynchronization in mild cognitive impairment: the 'X' model

Sandra Pusil,[1,2,*] María Eugenia López,[2,3,4,*] Pablo Cuesta,[2,5,*] Ricardo Bruña,[2,3,4] Ernesto Pereda[2,5] and Fernando Maestú[2,3,4]

[*]These authors contributed equally to this work.

Hypersynchronization has been proposed as a synaptic dysfunction biomarker in the Alzheimer's disease continuum, reflecting the alteration of the excitation/inhibition balance. While animal models have verified this idea extensively, there is still no clear evidence in humans. Here we test this hypothesis, evaluating the risk of conversion from mild cognitive impairment (MCI) to Alzheimer's disease in a longitudinal study. We compared the functional resting state eyes-closed magnetoencephalographic networks of 54 patients with MCI who were followed-up every 6 months. According to their clinical outcome, they were split into: (i) the 'progressive' MCI (n = 27) group; and (ii) the 'stable' MCI group (n = 27). They did not differ in gender or educational level. For all participants, two magnetoencephalographic recordings were acquired. Functional connectivity was evaluated using the phase locking value. To extract the functional connectivity network with significant changes between both magnetoencephalographic recordings, we evaluated the functional connectivity ratio, defined as functional connectivity post-/pre-condition, in a network-based statistical model with an ANCOVA test with age as covariate. Two significant networks were found in the theta and beta bands, involving fronto-temporal and fronto-occipital connections, and showing a diminished functional connectivity ratio in the progressive MCI group. These topologies were then evaluated at each condition showing that at baseline, patients with progressive MCI showed higher synchronization than patients with stable MCI, while in the post-condition this pattern was reversed. These results may be influenced by two main factors in the post-condition: the increased synchrony in the stable MCI patients and the network failure in the progressive MCI patients. These findings may be explained as an 'X' form model where the hypersynchrony predicts conversion, leading subsequently to a network breakdown in progressive MCI. Patients with stable MCI showed an opposite phenomenon, which could indicate that they were a step beyond in the Alzheimer's disease continuum. This model would be able to predict the risk for the conversion to dementia in MCI patients.

1 Laboratory of Neuropsychology, University of the Balearic Islands, Spain
2 Laboratory of Cognitive and Computational Neuroscience, Center for Biomedical Technology, Universidad Complutense and Universidad Politécnica de Madrid, Madrid, Spain
3 Department of Experimental Psychology, Universidad Complutense de Madrid, Madrid, Spain
4 Networking Research Center on Bioengineering, Biomaterials and Nanomedicine (CIBER-BBN), Madrid, Spain
5 Electrical Engineering and Bioengineering Lab, Department of Industrial Engineering and IUNE Universidad de La Laguna, Tenerife, Spain

Correspondence to: Sandra Pusil
Laboratory of Cognitive and Computational Neuroscience, Center for Biomedical Technology, Universidad Complutense and Universidad Politécnica de Madrid, 28223 Pozuelo de Alarcón, Madrid, Spain
E-mail: sandra.pusil@ctb.upm.es

Received February 8, 2019. Revised August 6, 2019. Accepted August 13, 2019

Keywords: stable and progressive mild cognitive impairment; functional connectivity; longitudinal study; magnetoencephalography; classification

Abbreviations: MEG = magnetoencephalography; p/sMCI = progressive/stable mild cognitive impairment

Introduction

Alzheimer's disease is a neurodegenerative disorder, which is clinically defined by a progressive loss of memory and other cognitive and functional abilities. It is considered the most common type of dementia, corresponding to ~60–80% of cases (Alzheimer's Association, 2016). The new inclusion of biomarkers by the National Institute on Aging-Alzheimer's Disease Association (NIA-AA), such as amyloid-β deposition or neuronal injury, has been considered an important advance to characterize the disease *in vivo* (McKhann *et al.*, 2011). However, the neuropathological and cognitive alterations that occur over the course of the disease are not as linear as commonly contemplated (Jack *et al.*, 2014). This enormous complexity makes the prediction regarding which individuals will finally progress to Alzheimer's disease difficult to answer.

Recent animal model studies have shown that during the Alzheimer's disease continuum, a cascade of biochemical and molecular changes produces a disruption of the excitation/inhibition balance (E/I balance), leading to the alteration of local and large-scale networks of the brain (Busche and Konnerth, 2016). One of the main pathological hallmarks of Alzheimer's disease, and largely responsible of the E/I imbalance, is amyloid-β deposition, which is primarily distributed over hippocampus and neocortex (Braak and Braak, 1991; Selkoe, 1991). Amyloid-β is primarily produced by the endocytosis of a transmembrane protein, amyloid precursor protein (APP), which modulates synapse formation and function (Priller *et al.*, 2006). APP inside the neuron increases the amyloid-β production that is secreted into the brain interstitial fluid. The accumulation of soluble amyloid-β within the interstitial fluid becomes abnormal during Alzheimer's disease as amyloid-β starts to aggregate into soluble amyloid-β oligomers and extracellular amyloid-β plaques (Cirrito *et al.*, 2005). Both amyloid-β forms exert a toxic effect on cells, causing the synaptic dysfunction that is a critical characteristic of the pathogenesis of Alzheimer's disease (Selkoe, 2002). In addition, in the vicinity of amyloid-β plaques, pyramidal neurons exhibit hyperactivity, possibly due to the lack of GABAergic perisomatic synapses (Garcia-Marin *et al.*, 2009). This increase of activity generates, in turn, an increment of the APP endocytosis, reinforcing the aberrant circle of amyloid-β production. This hyperactivity, mainly observed in earlier stages of the Alzheimer's disease continuum, is followed by a hypoactivity (Francis *et al.*, 1993; Palop and Mucke, 2010), which is characteristic of more advanced stages of the disease. For this reason Alzheimer's disease has been considered as a 'disconnection syndrome', not only because of the death of neurons and connections, but also because of the disruption of functional and structural brain networks (Delbeuck *et al.*, 2003).

With this background in mind, here we propose to test this E/I balance in a sample of subjects with mild cognitive impairment (MCI) from a longitudinal perspective. This symptomatic pre-dementia stage entails a higher risk of developing Alzheimer's disease (Jack *et al.*, 2011), being fundamental to the characterization of those profiles precluding dementia. To this end, we used magnetoencephalography (MEG), which is a non-invasive neuroimaging technique that directly measures the primary neural activity of the pyramidal neurons, allowing us to carry out follow-up studies of synaptic disruption (Stomrud *et al.*, 2010; Fernández *et al.*, 2013; López *et al.*, 2016). With the aim to explore long-range connections, we used functional connectivity (Friston, 1994), a measure that reflects the statistical interdependencies between two timeseries of physiological activity. In two previous studies carried out by our group (Bajo *et al.*, 2012; López *et al.*, 2014), we observed an increment of functional connectivity in those patients with MCI that progress to Alzheimer's disease [progressive (p)MCI] compared to those that remained stable [stable (s)MCI]. This hypersynchronization was also associated with the increased load of amyloid in the posterior regions (Nakamura *et al.*, 2017) and with the increased levels of p-tau in the CSF (Canuet *et al.*, 2015). These results show the hyperactivity previously explained in the animal model studies, but longitudinal studies with repeated measures are needed to track the time dynamics of this physiological phenomenon. Therefore, in the present study we followed-up a sample of MCI patients over a 3-year period, with their magnetic signals measured twice during this period. With the intent to better understand the relationship between connectivity changes and different features of Alzheimer's disease, we related functional connectivity results with cognitive (neuropsychological tests) and structural (medial temporal lobe volumes) information. Finally, we proposed an explanatory model—'X'—based — on our synchronization results, which describes how the E/I imbalance occurs during the disease, considering hypersynchronization as a marker of progression from MCI to Alzheimer's disease. To the best of our knowledge, repeated MEG measures together with this combination of variables have never been investigated in previous studies.

Materials and methods

Subjects

The initial sample of our study consisted of 145 MCI patients who were recruited from the Hospital Clínico Universitario

San Carlos (Madrid, Spain). Of this original sample, 54 were conscripted again for a second MEG scan after ~3 years (24 ± 6 months). They were all right-handed (Oldfield, 1971) and native Spanish speakers (see Table 1 for their demographic and clinical data).

All participants were screened with standardized diagnostic instruments and received an exhaustive neuropsychological assessment as previously described (López *et al.*, 2016). The MCI diagnosis was established according to the NIA-AA criteria (Albert *et al.*, 2011), which include: (i) self- or informant-reported cognitive complaints; (ii) objective evidence of impairment in one or more cognitive domains; (iii) preserved independence in functional abilities; and (iv) not demented (McKhann *et al.*, 2011). Besides meeting the clinical criteria, MCI participants had signs of neuronal injury (hippocampal volume measured by MRI). Therefore, they may be considered as 'MCI due to Alzheimer's disease' with an intermediate likelihood (Albert *et al.*, 2011). They were cognitively and clinically followed-up every 6 months and then split into two groups according to their clinical outcome: (i) the pMCI group (n = 27) was composed of those subjects that met the criteria for probable Alzheimer's disease (McKhann *et al.*, 2011); and (ii) the sMCI group (n = 27), composed of matching participants that still fulfilled the diagnosis criteria of MCI at the end of follow-up, and were randomly selected from the remaining 118 sMCI patients. The average time from first to second MEG was 27 ± 7 months for the sMCI group and 16 ± 9 months for the pMCI participants. In the pMCI group, the second MEG was performed when subjects progressed to Alzheimer's disease and, consequently, their follow-up time was shorter. Additionally, we included a group of 27 cognitively intact older adults as a reference to help the interpretation of the functional connectivity results obtained in the group comparison. The cognitively normal group was created mirroring the age, education and gender distribution of both MCI patient groups. The hippocampi volumes of the cognitively normal group were significantly higher (P-value < 0.05, ANCOVA test with age as covariate) than both MCI groups.

None of the participants had a history of psychiatric or neurological disorders (other than MCI or Alzheimer's disease). General inclusion criteria were: age between 65 and 80 years, a modified Hachinski score $\leqslant 4$, a short-form Geriatric Depression Scale score $\leqslant 5$, and T_1 MRI within 12 months and 2 weeks before the two MEG recordings without indication of infection, infarction, or focal lesions (rated by two independent experienced radiologists) (Bai *et al.*, 2012). Patients were OFF those medications that could affect MEG activity, such as benzodiazepines, 48 h before recordings.

The study was approved by the Hospital Universitario San Carlos Ethics Committee (Madrid), and all participants signed a written informed consent prior to participation.

Table 1 Mean ± SD values of the demographic and clinical characteristics of the sMCI and pMCI patients at pre-condition

	sMCI (n = 27)	pMCI (n = 27)	F-value	P-value
Age, years	71.23 ± 3.98	74.81 ± 3.98	2.6137	0.009*
Gender, females, n	15	18	Fisher's test	0.577
APOE genotype	12	13	Fisher's test	0.782
Education, years	8.88 ± 4.49	8.6 ± 4.49	0.0064	0.937
MMSE score	27.34 ± 3.39	25.95 ± 3.39	3.2289	0.079
MMSE (post-condition)	26.19 ± 4.13	23.65 ± 4.13	2.9490	0.092
Direct digit span	6.84 ± 2.28	7 ± 2.28	0.6555	0.422
Inverse digit span	4.46 ± 1.33	4.23 ± 1.33	0.1765	0.676
Immediate recall	19.34 ± 8.58	11.76 ± 8.58	5.5128	0.023*
Delayed recall	7.58 ± 4.98	2.76 ± 4.98	3.8756	0.055
Rule shift cards	2.16 ± 1.34	1.84 ± 1.34	0.0143	0.905
VOSP	6.83 ± 2.78	6.46 ± 2.78	0.0742	0.787
Phonemic fluency	8.2 ± 4.25	8.88 ± 4.25	0.1792	0.674
Semantic fluency	11.94 ± 3.99	11.96 ± 3.99	0.4430	0.509
TMTA (time)	82.86 ± 46.69	94.36 ± 46.69	0.6593	0.421
TMTB (time)	227.35 ± 127.84	254.95 ± 127.84	0.0194	0.890
Ideomotor praxis	7.29 ± 0.83	7.30 ± 0.83	0.4103	0.525
BNT	45.8 ± 9.01	44.65 ± 9.01	0.0730	0.788
BNT (phonemic)	6.33 ± 2.83	6.11 ± 2.83	0.0425	0.838
Hippocampal volume left	0.0024 ± 0.0003	0.0020 ± 0.0003	9.7773	0.003*
Hippocampal volume right	0.0025 ± 0.0003	0.0022 ± 0.0003	5.5714	0.023*
Entorhinal volume left	0.0014 ± 0.0005	0.0012 ± 0.0005	1.1795	0.284
Entorhinal volume right	0.0013 ± 0.0003	0.0013 ± 0.0003	1.7137	0.197
Parahippocampal volume left	0.0013 ± 0.0002	0.0013 ± 0.0002	1.1296	0.294
Parahippocampal volume right	0.0013 ± 0.0001	0.0012 ± 0.0001	4.6403	0.037*

BNT = Boston Naming Test; MMSE = Mini-Mental State Examination; TMTA = Trail-Making Test Part A; TMTB = Trail-Making Test Part B; VOSP = Visual Object and Space Perception Battery. P-values for between-group differences were introduced. *$P < 0.05$. Age differences were assessed with a Mann-Whitney test. An ANCOVA test, with age as a covariable, was used for continuous variables and Fisher's exact test for gender and *APOE* differences.

MRI and medial temporal lobe volumes

Three-dimensional T_1-weighted anatomical brain MRI scans were collected with a General Electric 1.5 T MRI scanner, using a high-resolution antenna and a homogenization PURE filter [fast spoiled gradient echo (FSPGR) sequence with parameters: repetition time/echo time/inversion time = 11.2/4.2/450 ms; flip angle 12°; 1 mm slice thickness, a 256 × 256 matrix and field of view 25 cm].

We used Freesurfer software (version 5.1.0.21) to obtain the medial temporal lobe volumes, which were normalized with the overall intracranial volume to account for differences in head volume over subjects.

MEG recordings

MEG signals were acquired using a whole-head Elekta-Neuromag MEG system with 306 channels (Elekta AB) at the Center for Biomedical Technology (Madrid, Spain). Data were collected at a sampling frequency of 1000 Hz and online band-pass filtered between 0.1 and 330 Hz.

MEG recordings were obtained at the same time of day in two different stages: (i) at baseline (pre-condition); and (ii) 24 ± 6 months (post-condition). The time between both MEG recordings was determined by the time of conversion to Alzheimer's disease in the pMCI patients, which was 16 ± 6 months. The MEG protocol consisted of 5 min at resting state with eyes closed. Subjects were seated comfortably inside a magnetically shielded room and were asked to relax and to reduce body movements. The positions of the four-head position indicator (HPI) coils attached to the scalp, and each subject's head shape relative to three anatomical locations (nasion and both preauricular points) was defined using a 3D digitizer (Fastrak). The subjects' head movements were continuously monitored by these HPI coils, and eye movements were monitored by the vertical electrooculograms with two pairs of bipolar electrodes. Raw recording data were first submitted to the Maxfilter software (v 2.2, correlation threshold = 0.9, time window = 10 s) to remove external noise with the temporal extension of the signal space separation method with movement compensation (Taulu and Simola, 2006). MEG data were automatically scanned for ocular, muscle and jump artefacts using the Fieldtrip software (Oostenveld *et al.*, 2011). Artefacts were then visually confirmed by an MEG expert. The remaining artefact-free data were segmented into 4-s segments (epochs). An independent component analysis-based procedure was used to remove the heart magnetic field artefact. Previous to source data calculation, MEG time series were filtered into theta (4.1–7.9 Hz), alpha (8.1–11.9 Hz), beta (12.1–29.9 Hz), and gamma (30.1–55.0 Hz) frequency bands with a 1500 order finite impulse response filter with Hamming window and a two-pass filtering procedure. Because of the high redundancy in MEG data after spatial filtering (Garcés *et al.*, 2017), we continued the analysis using only data from magnetometers.

Source reconstruction and connectivity analysis

A regular grid with 10 mm spacing was created in the template MNI. This set of nodes was transformed to each participant's space using a non-linear normalization between the native T_1 image (whose coordinate system was previously converted to match the MEG coordinate system) and a standard T_1 in MNI space. The forward model was solved with a single-shell method (Nolte, 2003) with a unique boundary defined by the inner skull (the combination of white matter, grey matter and CSF) taken from the individual T_1. Source reconstruction was carried out independently for each subject and frequency band, using a linearly constrained minimum variance (LCMV) beamformer (Van Veen *et al.*, 1997). Beamforming filters were estimated with normalized leadfields, regularized covariance matrices averaged over trials, and a 1% regularization factor. These neural MEG sources were anatomically parcellated by dividing the cortex into 72 regions of interest according to the AAL atlas (Tzourio-Mazoyer *et al.*, 2002). We selected the PCA as the representative time series for each brain area. Finally, the functional connectivity was assessed using the phase locking value (PLV), a phase synchronization measure that evaluates the distribution of phase differences extracted from each of two region of interest time series (Mormann *et al.*, 2000) and have demonstrated high reliability across sessions (Garcés *et al.*, 2016).

Statistical analyses

The PLV (post-condition/pre-condition) ratio was calculated to assess the change between the two conditions of the follow-up. These values were used to extract the networks that better differentiate both groups over time. The assessment of significant group functional connectivity differences was addressed relying on the network-based statistics (NBS) (Zalesky *et al.*, 2010; Fornito *et al.*, 2016), where the units of study were connected networks (set of nodes for which a link can be found between any pair of nodes in that network) in topological space. This procedure was applied independently for each frequency band. The methodology began by testing functional connectivity ratio differences between groups per each pair of regions of interest using an ANCOVA test while adjusting for the effects of age. The resulting matrix of F-statistics (with same dimension as the original functional connectivity matrix), was binarized by thresholding the matrix using a critical value computed with a *P*-value of 0.005. This binary matrix was split in two matrices attending to the sign of the differences between groups. A breadth-first search was used to identify connected components in each binary matrix. These connected components constituted the 'candidate networks of interest', also called a cluster in graph theory (Rubinov and Sporns, 2010). Candidate networks were required to have a minimum size defined by the obligation of involving at least 10% of the regions of interest of the model (i.e. seven regions of interest for our atlas model). Network mass statistics were assessed through the sum of all F-values corresponding to the network's links. Then, to control for the multiple comparison problem, this procedure was repeated 5000 times after shuffling the original group's labels. At each repetition, the maximum statistic of the surrogate networks was kept creating a maximal null distribution that ensured the control of the family-wise error rate (FWER) at the network level. The resulting NBS *P*-value for a candidate network corresponded with the proportion of the permutation distribution with network-statistic values greater than or equal to the network-statistic value of the original data. Only those

networks that survived the NBS at $P < 0.05$ or below were considered for the subsequent analyses as potential 'MEG markers'. As descriptive values for each significant network, we computed the average functional connectivity (across all links that belong to the network, i.e. their corresponding strength) for the functional connectivity ratio (pre- and post-functional connectivity values). These average functional connectivity values also calculated for the cognitively normal participants to obtain a reference value in the pre-condition. These values were used as functional connectivity marker values for the subsequent Spearman correlation analysis with neuropsychological scores and grey matter volumes. In addition, we computed pairwise statistics, between and within-groups, for these strength values using ANCOVA with age as covariate. Finally, to explore whether the MEG functional connectivity signatures could be useful in developing possible biomarkers of progression, a logistic regression classification analysis with a leave-one-out cross-validation procedure was carried out using network functional connectivity strength along with the medial temporal lobe volumes and the neuropsychological scores (López *et al.*, 2014*b*). Results were described in terms of accuracy, sensitivity, specificity, positive predictive value (PPV), and negative predictive value (NPV). Accuracy represents the fraction of subjects classified correctly. Sensitivity and specificity represent the fractions of pMCI and sMCI patients correctly classified, respectively. Finally, PPVs and NPVs represent the fraction of patients classified as pMCI that were really pMCI and the fraction of patients classified as sMCI that were really sMCI, respectively. Statistical analyses were carried out using MATLAB R2017b (Mathworks Inc) and all tests were two-tailed.

Data availability

The data that support the findings of this study are available from the corresponding author, upon reasonable request. All the algorithms used in the present paper are reported in the 'Materials and methods' section and in the Supplementary material.

Results

Functional connectivity ratio

The functional connectivity ratio was used to extract the network with a significant difference between both groups considering the information from both MEG recordings. The results showed two networks, in the theta and beta frequency bands, with a significantly diminished functional connectivity ratio in the pMCI patients when compared to the sMCI group. Although both frequency bands depicted the same overall behaviour, the band-specific topography of the networks differed. The theta band network mainly involved left frontal and occipital areas and right middle temporal regions (Fig. 1). On the other hand, the beta network appeared to be more lateralized to the right hemisphere (parieto-occipital regions) and connected with the left middle frontal gyrus (Fig. 2).

Pre and post-functional connectivity

The next step of the analysis consisted of the assessment of the specific topology of the functional connectivity ratio significant networks for each condition and group. Consequently, we explored the existence of significant differences between groups for each condition (sMCI/pre versus pMCI/pre and sMCI/post versus pMCI/post), and between-conditions within groups (sMCI/pre versus sMCI/post and pMCI/pre versus pMCI/post). We found that all pair-wise comparisons were significant (ANCOVA with age as covariate, P-value < 0.05) as shown in Fig. 3 (theta network) and Fig. 4 (beta network). In addition, when individual trajectories between both MEG recordings were depicted, the results showed that most participants behaved in a similar group manner. The sMCI patients showed an enhanced functional connectivity with time, whereas the pMCI individuals showed the opposite behaviour; their functional connectivity was diminished in the post-condition. When we assessed between-group comparisons within each condition, we found that the pMCI patients showed an enhanced functional connectivity when compared with the sMCI individuals at the pre-condition. Conversely, when the analysis was carried out with the functional connectivity values of the post-condition, the pMCI patients showed a diminished functional connectivity.

When the assessment of the specific topology of the functional connectivity ratio significant networks was carried out at the link level, the general profiles of Figs 3 and 4 emerged in both intra-condition analyses (Supplementary material). The pMCI group showed enhanced ipsilateral posterior functional connectivity in the pre-condition, whereas the sMCI group showed higher functional connectivity in the post-condition with a more anteriorized functional connectivity pattern. All links in the pre-condition displayed enhanced functional connectivity in the pMCI group when compared to sMCI participants. The opposite behaviour occurred in the post-condition. On the other hand, the results for the beta network displayed a similar behaviour; all links exhibited increased functional connectivity in the pMCI at the pre-condition, and decreased functional connectivity in the pMCI at the post-condition. Regarding the specific topology of the differences, we found that pMCI participants depicted higher antero-posterior functional connectivity in the pre-condition, whereas sMCI patients showed a hypersynchronized antero-posterior brain activity, when compared to the pMCI group, mostly contained in the right hemisphere.

Additionally, significant functional connectivity ratio differences (Figs 1 and 2) were further tested at the network (strength) and links level with extra ANCOVA tests with time and Mini-Mental State Evaluation (MMSE)-precondition score as covariates. These tests were carried out to distinguish whether the results could be influenced by these two potentially confounding factors. The results for the influence of difference in following time showed that 11

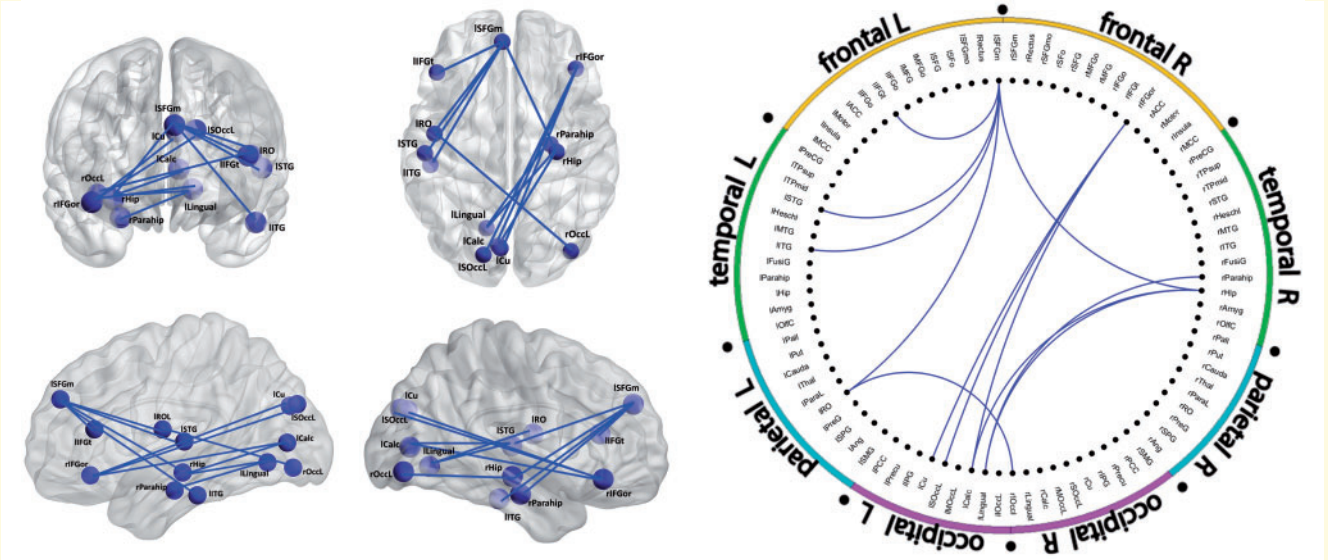

Figure 1 Functional connectivity ratio in theta band ($P < 0.005$). Blue links indicate pMCI < sMCI. (**A**) Coronal view; (**B**) axial view; (**C** and **D**) sagittal view left and right; and (**E**) circular connectivity diagram. lCalc = left calcarine; lCu = left cuneus; lIFGt = left inferior frontal gyrus triangular; lIFGt = left inferior frontal gyrus triangular part; lITG = left inferior temporal gyrus; lLingual = left lingual; lRO = left Rolandic; lSFGm = left superior frontal gyrus medial part; lSOccL = left superior occipital; lSTG = left superior temporal gyrus; rHip = right hippocampus; rIFGor = right inferior frontal gyrus orbital part; rOccL = right occipital; rParahip = right parahippocampus.

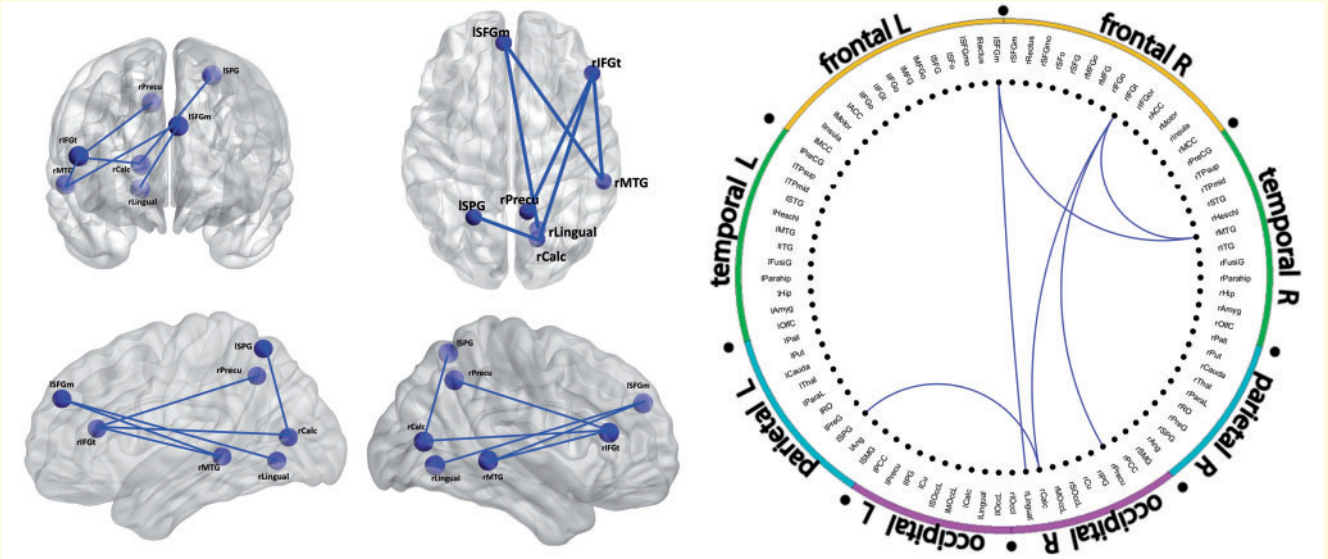

Figure 2 Functional connectivity ratio in beta band ($P < 0.005$). Blue links indicate pMCI < sMCI. (A) Coronal view; (B) axial view; (C and D) sagittal view left and right; and (E) circular connectivity diagram. lSFGm = left superior frontal gyrus medial part; lSP = left superior parietal gyrus; rCalc = right calcarine; rIFGt = right inferior frontal gyrus triangular part; rLingual = right lingual; rMTG = right middle temporal gyrus; rPrecu = right precuneus.

of 12 links of the theta network remained significant (lRO-lSFGm showed a *P*-value of 0.081). Similarly, five of six links of the beta network kept their significance (lSFGm-rMTG showed a *P*-value of 0.065). In both cases, the network strength remained highly significant. When the MMSE was evaluated, all links from both networks and both network strengths remained significant.

Finally, although this study is a longitudinal assessment aimed to extract those brain functional connectivity networks associated with deleterious changes over time in MCI patients that progressed to Alzheimer's disease, we included a cognitively normal group matched in age, sex and education with both MCI groups to provide reference functional connectivity values to better frame inter-MCI

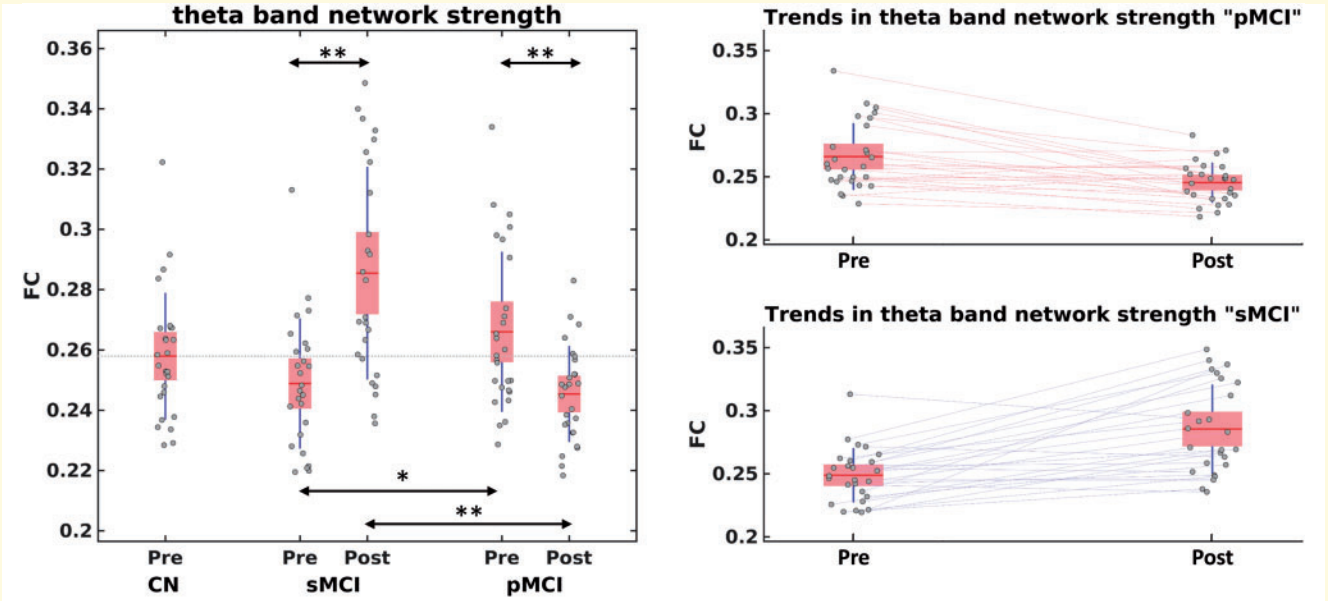

Figure 3 Analysis of the average functional connectivity of the theta functional connectivity ratio network topology for each condition and group. *Left*: Horizontal bars denote significant pairwise comparisons (*ANCOVA *P*-value < 0.05, **P-value < 0.0001). *Right*: Evolution of each participant, depicted within their corresponding group, along pre- and post- conditions. CN = cognitively normal; FC = functional connectivity.

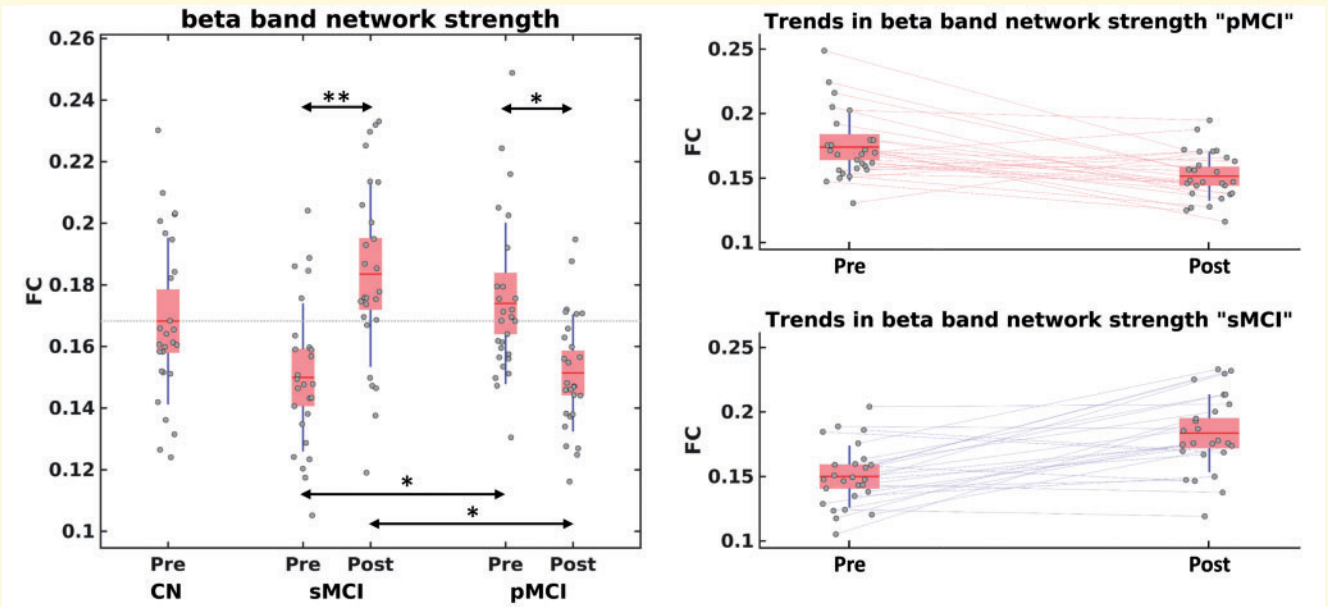

Figure 4 Analysis of the average functional connectivity of the beta functional connectivity ratio network topology for each condition and group. *Left*: Horizontal bars denote significant pairwise comparisons (*ANCOVA *P*-value < 0.001, **P-value < 0.0001). *Right*: Evolution of each participant, depicted within their corresponding group, along pre and post conditions. CN = cognitively normal; FC = functional connectivity.

functional connectivity differences. When the complete ratio network for the cognitively normal group (Figs 3 and 4) was compared to those corresponding to each MCI group in the pre-condition, only the beta functional connectivity (pre) of the sMCI patients showed significant differences (P-value < 0.05, ANCOVA test with age as covariate). The results for the post-condition showed that the cognitively normal group had lower functional connectivity than the sMCI group and higher functional connectivity than the pMCI group in the theta band. The result for the beta post-condition functional connectivity showed that cognitively normal participants presented higher functional

connectivity than pMCI patients. In addition, the comparison between cognitively normal and both MCI groups was performed at the links level. In both frequency bands, the results showed higher synchronization in the majority of these links in the pre-condition for the pMCI and hyposynchrony for the sMCI. The opposite pattern was shown for both frequency bands and most of the links in the post-condition.

Correlation between functional connectivity and medial temporal lobe volumes

The correlation analysis between functional connectivity values and neurophysiological and volumetric scores was carried out for the whole sample and for each group independently. This analysis was performed to explore possible relationships between our MEG signatures and multimodal information about participant's cognitive and structural status. Considering this aim, we reported any significant correlation ($P < 0.05$) using three different functional connectivity markers, on three different populations and for 24 scores. It is important to note that none of the correlations survived the FDR correction for multiple testing, but due to the exploratory character of this section of the analysis, and the quality of the scatters plots, we consider that the information is relevant and useful to the understanding of the neuroimaging markers. When all participants were included, we found significant results between the theta functional connectivity ratio and left hippocampal volume (rho = 0.351, *P*-value = 0.017), immediate recall (rho = 0.337, *P*-value = 0.015) and both MMSE scores (MMSE pre, rho = 0.283, *P*-value = 0.049; MMSE post, rho = 0.305, *P*-value = 0.028). On the other hand, the beta functional connectivity ratio correlated significantly with the left hippocampal volume (rho = 0.294, *P*-value = 0.048), the right hippocampal volume (rho = 0.360, *P*-value = 0.015) and the phonemic fluency performance (rho = −0.325, *P*-value = 0.019). The correlation analysis within the pMCI sample showed significant results (Fig. 5) only between the theta functional connectivity ratio and the inverse digit span (rho = 0.542, *P*-value = 0.004). Finally, in the case of the sMCI group (Fig. 5), the beta functional connectivity ratio correlated significantly with the right entorhinal volume (rho = −0.431, *P*-value = 0.036) and the phonemic fluency score (rho = −0.401, *P*-value = 0.042).

In addition to the functional connectivity ratio analysis, we carried out a similar analysis using the functional connectivity pre- and functional connectivity post-condition values in both groups separately. Results are displayed in Fig. 5 (top for pMCI group and bottom for the sMCI participants). In the pMCI group, the theta functional connectivity pre-condition correlated significantly with the delayed recall (rho = −0.442, *P*-value = 0.027), the theta functional connectivity post-condition correlated with the entorhinal volume (rho = 0.482, *P*-value = 0.025), and the beta functional connectivity pre-condition correlated with the right hippocampal volume (rho = −0.479, *P*-value = 0.025). On the other hand, in the sMCI group the beta functional connectivity pre-condition correlated with the direct digit span (rho = −0.448, *P*-value = 0.022), and the beta functional connectivity post-condition correlated with the phonemic fluency (rho = −0.458, *P*-value = 0.019).

Finally, as the follow-up time of the pMCI group corresponded with the time interval where their diagnosis was changed to Alzheimer's disease, we considered this time period as an upper boundary of the conversion time for pMCI patients. Then, we used a machine learning approach based on recursive partitioning (Breiman *et al.*, 1984), using the package 'rpart' in R, to study the influence of the sociodemographic variables, neuropsychological scores, MRI markers and functional connectivity markers in order to predict this estimate of the conversion time. The analysis selected functional connectivity markers together with medial temporal scores (both entorhinal and hippocampal volumes) as best predictors for the time to conversion. The model was able to explain 19.61% of the variance of the variable time of conversion. The importance of each variable in the prediction was the following: theta pre-condition functional connectivity (45%), left entorhinal (24%), right entorhinal (16%), sex (5%), beta pre-condition functional connectivity (5%), left hippocampus (3%), and MMSE pre-condition (2%).

Classification

The classification analysis assessed the utility of the functional connectivity markers to distinguish those patients who will progress to dementia. This analysis was carried out for each functional connectivity marker independently (to rank their individual capabilities as progression markers) and combined with the neuropsychological scores and the hippocampal volumes. All results are displayed in Table 2.

Regarding the functional connectivity markers, the best results for the functional connectivity values taking each one independently (Table 2), were obtained for the theta network ratio strength, which showed an accuracy of 83.0%. When both theta and beta network ratio strengths were used together in the classification the accuracy raised to 94.2%. If these two values were used in combination with the neurophysiological scores, inverse digit span and TMTA the accuracy reached 96.2% (the highest across all the classifications performed). Notwithstanding, the functional connectivity ratio requires two longitudinal points, so its use as a biomarker is limited. In that sense, both pre- and post-condition functional connectivity values would be better candidates. Using the pre-condition functional connectivity, we obtained an accuracy of 60% and 72% for the theta and beta bands, respectively, while for post-condition functional connectivity the accuracies were 77% for both frequency bands (Figs 3 and 4). When the pre-condition functional connectivity was combined with neurophysiological and volumetric scores, the best accuracy result of 79.2% was found for the assembly of both pre-condition functional

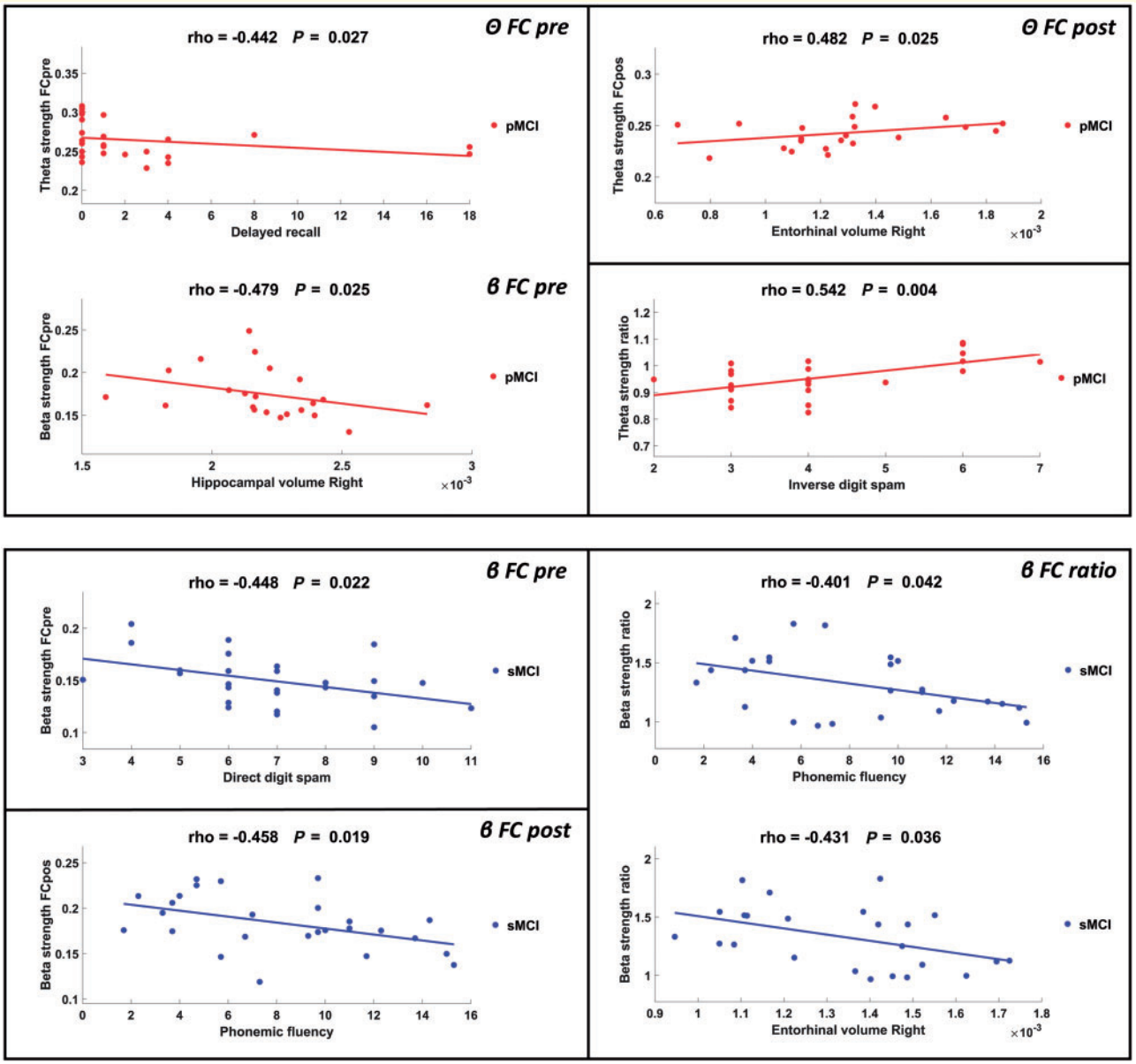

Figure 5 Correlations between functional connectivity and neuropyschological and volumetric scores. *Top*: Significant correlations (Spearman) between functional connectivity (FC) values and neurophysiological and volumetric scores in the progressive MCI population. *Bottom*: Significant correlations (Spearman) between functional connectivity values and neurophysiological and volumetric scores in the stable MCI population. Θ, β, FC, pre, post, ratio = theta or beta frequency band functional connectivity at pre-condition stage, post-condition stage, or ratio (post-condition/pre-condition), respectively.

connectivity strengths and the direct digit span and delayed recall scores. In the case of the post-condition functional connectivity the best result was found for the combination of both post-condition functional connectivity strength and the immediate recall and BNT (phonemic) scores, reaching an accuracy of 86.8% (Table 2).

Discussion

In recent years, the detection of those subjects with an increased risk of developing Alzheimer's disease has become an important issue in clinical neuroscience. Based on the idea developed in animal models that hypersynchronization (due to a loss of E/I balance) could be a sign of network disruption and increased brain pathology (Busche and Konnerth, 2016), we have tested these signs in those patients at higher risk of progression to Alzheimer's disease, namely a sample of patients with MCI. To this end, we assessed their brain functional networks at two different times. The sample comprised MCI patients divided into two subgroups: pMCI and sMCI. These two groups did differ in age, memory performance and hippocampi volumes, which are three relevant risk factors for developing

Table 2 Classification analysis

	Classification						
	Accuracy	Sens	Spec	PPV	NPV	Upper B	Lower B
Functional connectivity markers							
Theta ratio strength	0.830	0.889	0.769	0.800	0.870	0.919	0.702
Beta strength	0.792	0.815	0.769	0.786	0.800	0.892	0.659
Theta pre-FC strength	0.604	0.519	0.692	0.636	0.581	0.735	0.460
Beta pre-FC strength	0.717	0.667	0.769	0.750	0.690	0.832	0.577
Theta post-FC strength	0.774	0.852	0.692	0.742	0.818	0.877	0.638
Beta post-FC strength	0.774	0.741	0.808	0.800	0.750	0.877	0.638
Combination of scores							
Theta and beta ratio strengths	0.943	0.926	0.962	0.962	0.926	0.988	0.843
Theta and beta ratio strengths + inverse digit span + TMTA	0.962	0.926	1.000	1.000	0.929	0.995	0.870
Theta and beta pre-FC strengths	0.698	0.741	0.654	0.690	0.708	0.817	0.557
Theta and beta pre-FC strengths + Direct digit span + Delayed recall	0.792	0.778	0.808	0.808	0.778	0.892	0.659
Theta and beta post-FC strengths	0.792	0.852	0.731	0.767	0.826	0.892	0.659
Theta and beta post FC strengths + Immediate recall + BNT (phonemic)	0.868	0.852	0.885	0.885	0.852	0.945	0.747

Accuracy, sensitivity (Sens) and specificity (Spec), negative predictive value (NPV) and positive predictive value (PPV) scores were obtained through a logistic regression analysis with leave-one-out cross-validation procedure. The confidence interval (upper and lower B) (CI) for the statistic, were calculated using the β approach. BNT = Boston Naming Test; FC = functional connectivity; TMTA = Trail-Making Test Part A.

Alzheimer's disease (Lindsay *et al.*, 2002; Albert *et al.*, 2007; López *et al.*, 2014). According to these features, it may be argued that the pMCI patients could have already been predicted for their conversion to dementia. However, as we know from previous studies (Jack *et al.*, 2013), these three features alone do not provide enough specificity and sensitivity for predicting conversion from MCI to dementia. Several biomarkers are involved during the progression of the disease, making the individual diagnosis and its forecast a very complex task (Jack *et al.*, 2016, 2017). Therefore, tracking the place of each individual subject within the Alzheimer's disease continuum is one of the most important goals to be able to establish an accurate diagnosis and prognosis. To achieve this purpose, it is a priority to gather new information that could increase our predictive value, as well as explaining the neurophysiological basis of the disease. This was the aim of our longitudinal study. We aimed to characterize the functional changes of the brain along the Alzheimer's disease continuum in the same individuals, to provide new insights in the neuropathological process driven by the disease. By comparing these two MCI groups, it has allowed us to propose a model of progression from MCI to Alzheimer's disease based on our hyper- and hyposynchronization findings, called the 'X' model (Fig. 6).

The assessment of functional connectivity differences between both groups of MCI patients was carried out by means of the functional connectivity ratio between the functional connectivity values measured at post- and pre-conditions. The use of the functional connectivity ratio allowed us to focus on those links that were more affected by time and showed greater differences between both groups. We found two networks, one in the theta band and the other one in the beta band, where the functional connectivity ratio of the pMCI group was lower than that of the sMCI group. These networks involved the fronto-occipital cortex and fronto-temporal regions including the hippocampus. Moreover, the pMCI group functional connectivity ratio was found to be <1, indicating a decreased functional connectivity over time. On the other hand, the sMCI group had a functional connectivity ratio >1, suggesting an increased functional connectivity over time. This means that when the topologies of the significant networks

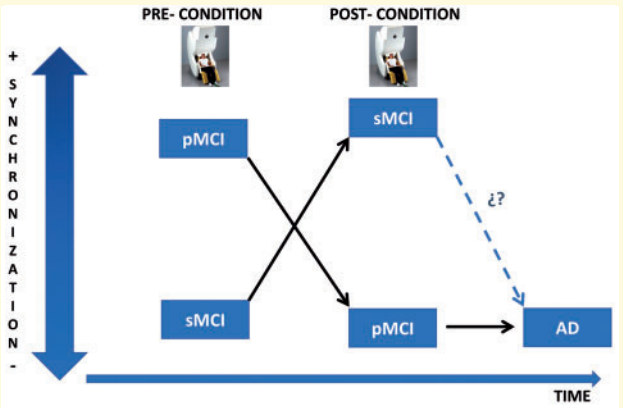

Figure 6 The 'X' model. The *x*-axis represents time, and the *y*-axis the synchronization (low values at the bottom, high levels at the top). In the pre-condition (when both groups are diagnosed as MCI), the pMCI group exhibits higher synchronization values than the sMCI group, but in the post-condition (when the pMCI patients have converted to Alzheimer's disease), they exhibit lower levels than the sMCI patients. It would be hypothesized that those with sMCI who finally progress to Alzheimer's disease will exhibit higher synchronization values before progressing to the Alzheimer's disease condition, when their synchronization will fall (represented by the dashed line and the question mark). AD = Alzheimer's disease.

were assessed at each condition, the pMCI group presented higher functional connectivity at baseline and a lower functional connectivity after 3 years of follow-up than the sMCI group. These results mirrored previous findings from our group, obtained in an independent sample, where we found an increased fronto-hippocampal connectivity in MCI patients with high levels of p-tau in their CSF (Canuet *et al.*, 2015), and an increased fronto-occipital connectivity in MCI patients progressing to dementia (López *et al.*, 2014). Additionally, the time-related decrement of functional connectivity in the pMCI could be seen as unusual as most studies have found an increase in the power of slow activity in MCI and Alzheimer's disease patients (Stam, 2010; Babiloni *et al.*, 2011). However, some studies that used attentional and memory task-related paradigms, found a significant reduction in theta functional connectivity in pMCI patients compared to sMCI patients (Güntekin *et al.*, 2008; Deiber *et al.*, 2009; Missonnier *et al.*, 2010; Wang *et al.*, 2014). In addition, theta oscillations are usually involved in working memory activity (Sarnthein *et al.*, 1998; Anokhin *et al.*, 1999; Stam, 2000), involving the medial prefrontal region (Gevins *et al.*, 1997; Raghavachari *et al.*, 2001), which is typically a brain region with high amyloid accumulation in Alzheimer's disease patients. Furthermore, beta band seems to have a special significance in Alzheimer's disease, especially in the early stages of the disease (Stam *et al.*, 2003). This band has been classically related to excitatory activity, as well as to cognitive processes impaired in Alzheimer's disease, such as memory or executive function (Koenig *et al.*, 2005). Our results agree with those obtained by Koenig *et al.* (2005), who described that beta band synchronization was lower in Alzheimer's disease than in MCI subjects, and those reported by Koelewijn *et al.* (2017), which found a decreased resting state MEG functional connectivity in Alzheimer's disease patients compared to healthy older subjects.

Thus, this approach gave us a brain network profile and a related underlying neurophysiological process predicting the conversion, or not, to Alzheimer's disease within the time period between the two MEG recordings. This idea was reinforced by the correlation analysis, showing an association between the hypersynchronization and the worsening of the cognitive functions.

Regarding the results found in the correlation analyses with the neuropsychological scores and medial temporal volumes obtained at the pre-condition, when the whole sample was taken into account, the functional connectivity ratio correlated positively with cognitive and structural information. The higher the increase of post-condition functional connectivity in comparison with pre-condition functional connectivity, the better cognitive performance (immediate recall and MMSE pre- and post-condition scores) and the bigger the hippocampal volumes. This relationship confirms that functional disruptions of these fronto-temporal networks may be related to episodic memory, both anatomically and functionally, which is one of the main hallmarks of Alzheimer's disease (Sperling *et al.*, 2010; López *et al.*, 2014; Canuet *et al.*, 2015). Notwithstanding, we are aware that these results should be affected to some extent by a circularity problem. Indeed, both groups significantly differed in hippocampal volumes and memory, and the functional connectivity ratio values were found by exploring the differences between both groups. To avoid this effect, we computed the correlation analyses at the single population level finding that, in the pMCI group, the theta functional connectivity ratio was positively correlated to inverse digit span, whereas the beta functional connectivity ratio in the sMCI group was inversely associated with phonemic fluency and entorhinal volume. These results mainly suggest that executive functions are more affected with the progression of the disease, characterized by a reduction of synchronization over time.

Ratios between pre- and post-conditions provide general profiles of the functional connectivity tendencies across time. However, to evaluate group differences at each time evaluated (pre- and post-conditions) we compared functional connectivity profiles separately. In line with the above, pMCI presents a higher functional connectivity compared to the sMCI group in the pre-condition, i.e. when all participants fulfilled the diagnosis of MCI. This pattern of hypersynchronization has previously been observed in some MEG studies. For instance, Bajo *et al.* (2012) reported that pMCI patients showed higher values of synchronization over parieto-occipital sensors in the alpha and beta-1 bands than sMCI patients during the performance of a short-term memory task. López *et al.* (2014) found, in a resting-state study, that the pMCI group exhibited a higher synchronization in the alpha band between the right anterior cingulate and temporo-occipital regions than sMCI subjects. Finally, Canuet *et al.* (2015) found increased fronto-hippocampal synchronization in the presence of high p-tau in the CSF in patients who converted to dementia late. This increased synchronization observed in pMCI patients can be interpreted from two different points of view. Classically, it has been explained as the result of a mechanism of compensation, in which additional networks increase their role to overcome the inefficiency of those networks that do not work as well (Bajo *et al.*, 2010; Liang *et al.*, 2011; Clément and Belleville, 2012; Abuhassan *et al.*, 2014). However, we may speculate that the profile of hypersynchronization found here, as in other studies, may be related to the pathological process of Alzheimer's disease (de Haan *et al.*, *2012a*, *b*; López *et al.*, 2014). This view of synchronization as a pathological sign, not as compensatory, would reflect the hyperexcitability of the pyramidal neurons induced by the lack of inhibitory connections caused by the toxic effects of the neuritic plaques as previously shown in animal models (Cirrito *et al.*, 2005; Garcia-Marin *et al.*, 2009). Thus, the greater the neuronal excitability, the greater the likelihood of neuronal synchronization, which may lead to the establishment of aberrant relationships between brain areas.

On the other hand, in the post-condition, the pMCI group showed a significantly decreased functional

connectivity when compared to the sMCI group. This decrease in functional connectivity has previously been observed in Alzheimer's disease patients, being considered as a sign of network breakdown (Wang *et al.*, 2013, 2014; Garcés *et al.*, 2014; Canuet *et al.*, 2015; Jones *et al.*, 2016), representing a loss of network robustness and a deviation from the optimal configuration of the brain dynamic processing that occurs during the progression of the disease (Engels *et al.*, 2015; Zhou *et al.*, 2015). These results may confirm what we speculated in our previous longitudinal study (López *et al.*, 2014). As the disease progresses, the hypersynchronization observed in the pMCI group would cause neuronal death due to excessive calcium-mediated activity (de Haan *et al.*, 2012*a*, *b*), leading to the characteristic network disruption observed in more advanced stages of Alzheimer's disease (Locatelli *et al.*, 1998; Koenig *et al.*, 2005; Stam *et al.*, 2009).

In addition, the sMCI group behaved in a similar fashion to the pMCI group, but delayed in time, that is, they showed less connectivity than the pMCI in the pre-condition, because their status was probably not as advanced as the pMCI. However, in the post-condition, this group exhibited an increase in brain connectivity showing the characteristic hypersynchronization pattern of the pMCI patients at the pre-condition. We can speculate that this increased synchronization for the sMCI group in the post-condition may reflect an increased neurophysiological risk status for developing dementia.

Based on our previous (Bajo *et al.*, 2012; López *et al.*, 2014) and present functional connectivity findings, we propose the 'X' model (Fig. 6), in which higher synchronization values in the pre-condition are related to the progression to Alzheimer's disease, while the opposite pattern would be associated with a stable diagnosis of MCI. On the contrary, lower synchronization values in the post-condition are related to the Alzheimer's disease status, as seen in the pMCI group, whereas higher synchronization values are related with the sMCI group, that will probably suffer dementia in the future (and will then exhibit decreased synchronization when they become Alzheimer's disease patients, as in the pMCI group in the post-condition). Thus, the 'X' model would support the evidence of the disruption of the E/I balance found in animal model studies, which would lead to the alteration of the synchronization of brain networks during the continuum of the disease. Within this E/I imbalance, it seems clear that the hypersynchronization would precede the conversion from MCI to Alzheimer's disease, and therefore it could be considered as a biomarker for the increased risk for the development of dementia. To test this hypothesis of hypersynchronization as a conversion marker, future studies should include the followed-up sMCI subjects who showed this pattern.

The 'X' model may be supported by the results obtained from the correlation analyses, where those pMCI subjects who exhibited greater structural and cognitive alterations presented higher pre-condition functional connectivity and lower functional connectivity post-condition. These results would confirm the idea that the hypersynchronization is linked to a cognitive and morphological decline reflecting a sign of disease and not a compensatory activity. On the other hand, those sMCI patients that showed lower cognitive scores and lower hippocampal volumes exhibited as hypersynchronization in both conditions. This finding could be due to the unknown information regarding the pathological evolution of these subjects. For this reason, we hypothesized that those sMCI participants with higher synchronization values and lower structural and cognitive scores may be more at risk to finally develop Alzheimer's disease in a short period of time.

Finally, in our aim to delineate an integrative approach of the impact that functional connectivity, neuropsychological and anatomical information may exert in the progression from MCI to Alzheimer's disease, we built a classification model by using these three variables as factors. It is important to note that several studies have focused on the conversion from MCI to Alzheimer's disease from different perspectives, suggesting the involvement of different frequency bands as markers of conversion (Poil *et al.*, 2013; Gallego-Jutglà *et al.*, 2014; Al-Jumeily *et al.*, 2015). Nevertheless, the combination of marker results are very useful for these models to gain predictive capability (Modrego, 2006; Antila *et al.*, 2013; López *et al.*, 2016). Thus, the proposed predictive model with higher classification values includes both theta and beta bands, average functional connectivity ratios and two neuropsychological scores: TMTA (time) and inverse digit span, which are often related to working memory, attentional and executive functions. The inclusion of all of these variables allowed an accuracy of 96.2% (Table 2). These extra memory cognitive impairments seem to play a role in the prediction of Alzheimer's disease (Chapman *et al.*, 2012; López *et al.*, 2014). But, in order to provide a classification with a clinical utility, we also created a model based on the pre-condition variables. Thus, we found an accuracy of 79.2% to discriminate between pMCI and sMCI with the average pre-condition functional connectivity of the significant networks in theta and beta bands, the direct digit span and the delayed recall. These findings suggest that the network disruption and the neuropsychological scores related to memory are good predictors to distinguish between groups.

Brain connectivity allows us a better understanding of brain functioning and how the disease causes network disruption and consequently affects the cognitive status of the patients (de Haan *et al.*, 2012*a*, *b*). Therefore, the present work provides a new model to study the evolution of Alzheimer's disease and supports the neurophysiological profiles as an important biomarker to evaluate the alterations caused by synaptic disruption during the course of this disease and to establish predictions on its course.

The main limitations of our study are as follows: (i) evidence regarding the diagnosis of our sample is based on neuronal injury (measured by MRI) and clinical criteria, but we do not provide cerebrospinal markers and/or amyloid accumulation measured by PET. However, we

established very strict inclusion criteria and clinically followed-up all samples, which ensured that only MCI due to Alzheimer's disease patients were included in the study. (ii) We did not carry out a third MEG scan of the sMCI sample, information that would be needed to test our model. However, future studies will shed light on the hypersynchronization as a marker of progression from MCI to Alzheimer's disease based on their synchronization profiles. According to our results, we will predict that those sMCI patients with higher PLV values in the post-condition will progress to dementia in the short or medium term. Another way to test the 'X' model would be to see whether patients under pharmacological and non-pharmacological interventions would show different trajectories than the ones predicted in our model. It is interesting to say that these profiles of synchronization can also be computed with EEG, making it possible to be tested in larger populations of elderly subjects.

Acknowledgements

We sincerely thank all the researchers at the Laboratory for Cognitive and Computational Neuroscience (LNCyC) at the Center for Biomedical Technology in Madrid. We also thank all clinical doctors and staff at Hospital Clínico Universitario San Carlos in Madrid. Finally, we are deeply indebted to all the research patients and their supporters without whom this work would not have been possible.

Funding

This study was supported by three projects from the Spanish Ministry of Economy and Competitiveness (PSI2009-14415-C03-01, PSI2012-38375-C03-01, and TEC2016-80063-C3-2-R) and from Madrid Neurocenter (B2017/BMD-3760). Complementary, it was supported by a post-doctoral fellowship from the Spanish Ministry of Economy and Competitiveness to Sandra Pusil (BES-2014-069501), and to Pablo Cuesta (FJCI-2015-26755).

Competing interests

The authors report no competing interest. The funding sources had no role in the study design, data collection, data analyses, or data interpretation.

Supplementary material

Supplementary material is available at *Brain* online.

References

Abuhassan K, Coyle D, Belatreche A, Maguire L. Compensating for synaptic loss in Alzheimer's disease. J Comput Neurosci 2014; 36: 19–37.

Al-Jumeily D, Iram S, Vialatte F-B, Fergus P, Hussain A. A novel method of early diagnosis of Alzheimer's disease based on EEG signals. Sci World J 2015;2015: 1–11.

Albert M, Moss MB, Blacker D, Tanzi R, McArdle JJ. Longitudinal change in cognitive performance among individuals with mild cognitive impairment. Neuropsychology 2007; 21: 158–69.

Albert MS, DeKosky ST, Dickson D, Dubois B, Feldman HH, Fox NC, et al. The diagnosis of mild cognitive impairment due to Alzheimer's disease: recommendations from the National Institute on Aging-Alzheimer's Association workgroups on diagnostic guidelines for Alzheimer's disease. Alzheimers Dement 2011; 7: 270–9.

Alzheimer's Association. 2016 Alzheimer's disease facts and figures. Alzheimers Dement 2016; 12: 459–509.

Anokhin AP, Lutzenberger W, Birbaumer N. Spatiotemporal organization of brain dynamics and intelligence: an EEG study in adolescents. Int J Psychophysiol 1999; 33: 259–73.

Antila K, Lötjönen J, Thurfjell L, Laine J, Massimini M, Rueckert D, et al. The PredictAD project: development of novel biomarkers and analysis software for early diagnosis of the Alzheimer's disease The PredictAD project: development of novel biomarkers and analysis software for early diagnosis of the Alzheimer's disease 2013; Interface Focus 2013; 3: 20120072.

Babiloni C, Vecchio F, Lizio R, Ferri R, Rodriguez G, Marzano N, et al. Resting state cortical rhythms in mild cognitive impairment and Alzheimer's disease: electroencephalographic evidence. Adv Alzheimer's Dis 2011; 2: 391–404.

Bai Y, Hu Y, Wu Y, Zhu Y, He Q, Jiang C, et al. A prospective, randomized, single-blinded trial on the effect of early rehabilitation on daily activities and motor function of patients with hemorrhagic stroke. J Clin Neurosci 2012; 19: 1376–9.

Bajo R, Castellanos NP, Cuesta P, Aurtenetxe S, Garcia-Prieto J, Gil-Gregorio P, et al. Differential patterns of connectivity in progressive mild cognitive impairment. Brain Connect 2012; 2: 21–4.

Bajo R, Maestú F, Nevado A, Sancho M, Gutiérrez R, Campo P, et al. Functional connectivity in mild cognitive impairment during a memory task: implications for the disconnection hypothesis. J Alzheimers Dis 2010; 22: 183–93.

Braak H, Braak E. Demonstration of amyloid deposits and neurofibrillary changes in whole brain sections. Brain Pathol 1991; 1: 213–6.

Breiman L, Friedman J, Stone CJ, Olshen RA. Classification and regression trees. Boca Raton: Chapman and Hall/CRC;1984.

Busche MA, Konnerth A. Impairments of neural circuit function in Alzheimer's disease. Philos Trans R Soc London-Ser B Biol Sci 2016; 371: 1–10.

Canuet L, Pusil S, López ME, Bajo R, Pineda-Pardo JÁ, Cuesta P, et al. Network disruption and cerebrospinal fluid amyloid-beta and phospho-tau levels in mild cognitive impairment. J Neurosci 2015; 35: 10325–30.

Chapman RM, Mapstone M, Mccrary JW, Gardner MN, Porsteinsson A, Sandoval TC, et al. Predicting conversion from Mild cognitive impairment to Alzheimer's Disease using neuropsychological test and multivariate methods. J Clin Exp Neuropsychol 2012; 33: 187–99.

Cirrito JR, Yamada KA, Finn MB, Sloviter RS, Bales KR, May PC, et al. Synaptic activity regulates interstitial fluid amyloid-beta levels in vivo. Neuron 2005; 48: 913–22.

Clément F, Belleville S. Effect of disease severity on neural compensation of item and associative recognition in mild cognitive impairment. J Alzheimers Dis 2012; 29: 109–23.

de Haan W, Mott K, van Straaten ECW, Scheltens P, Stam CJ. Activity dependent degeneration explains hub vulnerability in Alzheimer's disease. PLoS Comput Biol 2012a; 8: e1002582.

de Haan W, Van der Flier WM, Koene T, Smits LL, Scheltens P, Stam CJ. Disrupted modular brain dynamics reflect cognitive dysfunction in Alzheimer's disease. Neuroimage 2012b; 59: 3085–93.

Deiber M-P, Ibañez V, Missonnier P, Herrmann F, Fazio-Costa L, Gold G, et al. Abnormal-induced theta activity supports early directed-attention network deficits in progressive MCI. Neurobiol Aging 2009; 30: 1444–52.

Delbeuck X, Van der Linden M, Collette F. Alzheimer's disease as a disconnection syndrome? Neuropsychol Rev 2003; 13: 79–92.
Engels MM, Stam CJ, van der Flier WM, Scheltens P, de Waal H, van Straaten EC. Declining functional connectivity and changing hub locations in Alzheimer's disease: an EEG study. BMC Neurol 2015; 15: 145.
Fernández A, Turrero A, Zuluaga P, Gil-Gregorio P, Del Pozo F, Maestu F, et al. MEG delta mapping along the healthy aging-alzheimer's disease continuum: diagnostic implications. J Alzheimer's Dis 2013; 35: 495–507.
Fornito A, Zalesky A, Bullmore ET. Fundamentals of brain network analysis. London: Elsevier;2016.
Francis PT, Sims NR, Procter AW, Bowen DM. Cortical pyramidal neurone loss may cause glutamatergic hypoactivity and cognitive impairment in Alzheimer's disease: investigative and therapeutic perspectives. J Neurochem 1993; 60: 1589–604.
Friston KJ. Functional and effective connectivity in neuroimaging: a synthesis. Hum Brain Mapp 1994; 2: 56–78.
Gallego-Jutglà E, Solé-Casals J, Vialatte F-B, Dauwels J, Cichocki A. A theta-band EEG based index for early diagnosis of Alzheimer's disease. J Alzheimers Dis 2014; 43: 1175–84.
Garcés P, Angel Pineda-Pardo J, Canuet L, Aurtenetxe S, López ME, Marcos A, et al. The default mode network is functionally and structurally disrupted in amnestic mild cognitive impairment-a bimodal MEG-DTI study. NeuroImage Clin 2014; 6: 214–21.
Garcés P, López-Sanz D, Maestú F, Pereda E. Choice of magnetometers and gradiometers after signal space separation. Sensors (Switzerland) 2017; 17: 2926.
Garcés P, Martín-Buro MC, Maestú F. Quantifying the test-retest reliability of magnetoencephalography resting-state functional connectivity. Brain Connect 2016; 6: 448–60.
Garcia-Marin V, Blazquez-Llorca L, Rodriguez J-R, Boluda S, Muntane G, Ferrer I, et al. Diminished perisomatic GABAergic terminals on cortical neurons adjacent to amyloid plaques. Front Neuroanat 2009; 3: 28.
Gevins A, Smith ME, McEvoy L, Yu D. High-resolution EEG mapping of cortical activation related to working memory: effects of task difficulty, type of processing, and practice. Cereb Cortex 1997; 7: 374–85.
Güntekin B, Saatçi E, Yener G. Decrease of evoked delta, theta and alpha coherences in Alzheimer patients during a visual oddball paradigm. Brain Res 2008; 1235: 109–16.
Jack CR, Albert MS, Knopman DS, McKhann GM, Sperling RA, Carrillo MC, et al. Introduction to the recommendations from the National Institute on Aging-Alzheimer's Association workgroups on diagnostic guidelines for Alzheimer's disease. Alzheimers Dement 2011; 7: 257–62.
Jack CR, Knopman DS, Jagust WJ, Petersen RC, Weiner MW, Aisen PS, et al. Tracking pathophysiological processes in Alzheimer's disease: an updated hypothetical model of dynamic biomarkers. Lancet Neurol 2013; 12: 207–16.
Jack CR, Therneau TM, Wiste HJ, Weigand SD, Knopman DS, Lowe VJ, et al. Transition rates between amyloid and neurodegeneration biomarker states and to dementia: a population-based, longitudinal cohort study. Lancet Neurol.2016; 15: 56–64.
Jack CR, Wiste HJ, Knopman DS, Vemuri P, Mielke MM, Weigand SD, et al. Rates of β-amyloid accumulation are independent of hippocampal neurodegeneration. Neurology 2014; 82: 1605–12.
Jack CR, Wiste HJ, Weigand SD, Therneau TM, Knopman DS, Lowe V, et al. Age-specific and sex-specific prevalence of cerebral β-amyloidosis, tauopathy, and neurodegeneration in cognitively unimpaired individuals aged 50–95 years: a cross-sectional study. Lancet Neurol 2017; 16: 435–44.
Jones DT, Knopman DS, Gunter JL, Graff-Radford J, Vemuri P, Boeve BF, et al. Cascading network failure across the Alzheimer's disease spectrum. Brain 2016; 139: 547–62.
Koelewijn L, Bompas A, Tales A, Brookes MJ, Muthukumaraswamy SD, Bayer A, et al. Clinical neurophysiology Alzheimer's disease disrupts alpha and beta-band resting-state oscillatory network connectivity. Clin Neurophysiol 2017; 128: 2347–57.
Koenig T, Prichep L, Dierks T, Hubl D, Wahlund LO, John ER, et al. Decreased EEG synchronization in Alzheimer's disease and mild cognitive impairment. Neurobiol Aging 2005; 26: 165–71.
Liang P, Wang Z, Yang Y, Jia X, Li K. Functional disconnection and compensation in mild cognitive impairment: evidence from DLPFC connectivity using resting-state fMRI. PLoS One 2011; 6: e22153.
Lindsay J, Laurin D, Verreault R, Hébert R, Helliwell B, Hill GB, et al. Risk factors for Alzheimer's disease: a prospective analysis from the canadian study of health and aging. Am J Epidemiol 2002; 156: 445–53.
Locatelli T, Cursi M, Liberati D, Franceschi M, Comi G. EEG coherence in Alzheimer's disease. Electroencephalogr Clin Neurophysiol 1998; 106: 229–37.
López ME, Bruña R, Aurtenetxe S, Pineda-Pardo JÁ, Marcos A, Arrazola J, et al. Alpha-band hypersynchronization in progressive mild cognitive impairment: a magnetoencephalography study. J Neurosci 2014; 34: 14551–9.
López MEME, Turrero A, Cuesta P, López-Sanz D, Bruña R, Marcos A, et al. Searching for primary predictors of conversion from mild cognitive impairment to Alzheimer's disease: a multivariate follow-up study. J Alzheimer's Dis 2016; 52: 133–43.
McKhann GM, Knopman DS, Chertkow H, Hyman BT, Jack CR, Kawas CH, et al. The diagnosis of dementia due to Alzheimer's disease: recommendations from the National Institute on Aging-Alzheimer's Association workgroups on diagnostic guidelines for Alzheimer's disease. Alzheimer's Dement 2011; 7: 263–9.
Missonnier P, Herrmann FR, Michon A, Fazio-Costa L, Gold G, Giannakopoulos P. Early disturbances of gamma band dynamics in mild cognitive impairment. J Neural Transm 2010; 117: 489–98.
Modrego PJ. Predictors of conversion to dementia of probable Alzheimer type in patients with mild cognitive impairment. Curr Alzheimer Res 2006; 3: 161–70.
Mormann F, Lehnertz K, David P, E. Elger C. Mean phase coherence as a measure for phase synchronization and its application to the EEG of epilepsy patients. Physica D 2000; 144: 358–69.
Nakamura A, Cuesta P, Kato T, Arahata Y, Iwata K, Yamagishi M, et al. Early functional network alterations in asymptomatic elders at risk for Alzheimer's disease. Sci Rep 2017; 7: 6517.
Nolte G. The magnetic lead field theorem in the quasi-static approximation and its use for magnetoencephalography forward calculation in realistic volume conductors. Phys Med Biol 2003; 48: 3637–52.
Oldfield RC. The assessment and analysis of handedness: the Edinburgh inventory. Neuropsychologia 1971; 9: 97–113.
Oostenveld R, Fries P, Maris E, Schoffelen J-M. FieldTrip: Open source software for advanced analysis of MEG, EEG, and invasive electrophysiological data. Comput Intell Neurosci 2011;2011: 156869.
Palop JJ, Mucke L. Amyloid-β–induced neuronal dysfunction in Alzheimer's disease: from synapses toward neural networks. Nat Neurosci 2010; 13: 812–8.
Poil SS, de Haan W, van der Flier WM, Mansvelder HD, Scheltens P, Linkenkaer-Hansen K. Integrative EEG biomarkers predict progression to Alzheimer's disease at the MCI stage. Front Aging Neurosci 2013; 5: 1–12.
Priller C, Bauer T, Mitteregger G, Krebs B, Kretzschmar HA, Herms J. Synapse formation and function is modulated by the amyloid precursor protein. J Neurosci 2006; 26: 7212–21.
Raghavachari S, Kahana MJ, Rizzuto DS, Caplan JB, Kirschen MP, Bourgeois B, et al. Gating of human theta oscillations by a working memory task. J Neurosci 2001; 21: 3175–83.
Rubinov M, Sporns O. Complex network measures of brain connectivity: uses and interpretations. Neuroimage 2010; 52: 1059–69.
Sarnthein J, Petsche H, Rappelsberger P, Shaw GL, von Stein A. Synchronization between prefrontal and posterior association cortex during human working memory. Proc Natl Acad Sci U S A 1998; 95: 7092–6.

Selkoe DJ. The molecular pathology of Alzheimer's disease. Neuron 1991; 6: 487–98.
Selkoe DJ. Alzheimer's disease is a synaptic failure. Science 2002; 298: 789–91.
Sperling R, Dickerson B, Pihlajamaki M, Vannini P, LaViolette P, Vitolo O, et al. Functional alterations in memory networks in early Alzheimer's disease. Neuromol Med 2010; 12: 27–43.
Stam CJ. Brain dynamics in theta and alpha frequency bands and working memory performance in humans. Neurosci Lett 2000; 286: 115–8.
Stam CJ. Use of magnetoencephalography (MEG) to study functional brain networks in neurodegenerative disorders. J Neurol Sci 2010; 289: 128–34.
Stam CJ, de Haan W, Daffertshofer A, Jones BF, Manshanden I, van Cappellen van Walsum AM, et al. Graph theoretical analysis of magnetoencephalographic functional connectivity in Alzheimer's disease. Brain 2009; 132: 213–24.
Stam CJ, van der Made Y, Pijnenburg YAL, Scheltens P. EEG synchronization in mild cognitive impairment and Alzheimer's disease. Acta Neurol Scand 2003; 108: 90–6.
Stomrud E, Hansson O, Minthon L, Blennow K, Rosén I, Londos E. Slowing of EEG correlates with CSF biomarkers and reduced cognitive speed in elderly with normal cognition over 4 years. Neurobiol Aging 2010; 31: 215–23.
Taulu S, Simola J. Spatiotemporal signal space separation method for rejecting nearby interference in MEG measurements. Phys Med Biol 2006; 51: 1759–68.
Tzourio-Mazoyer N, Landeau B, Papathanassiou D, Crivello F, Etard O, Delcroix N, et al. Automated anatomical labeling of activations in SPM using a macroscopic anatomical parcellation of the MNI MRI single-subject brain. Neuroimage 2002; 15: 273–89.
Van Veen BD, van Drongelen W, Yuchtman M, Suzuki A. Localization of brain electrical activity via linearly constrained minimum variance spatial filtering. IEEE Trans Biomed Eng 1997; 44: 867–80.
Wang J, Zuo X, Dai Z, Xia M, Zhao Z, Zhao X, et al. Disrupted functional brain connectome in individuals at risk for Alzheimer's disease. Biol Psychiatry 2013; 73: 472–81.
Wang R, Wang J, Yu H, Wei X, Yang C, Deng B. Decreased coherence and functional connectivity of electroencephalograph in Alzheimer's disease. Chaos 2014; 24: 033136.
Zalesky A, Fornito A, Bullmore ET. Network-based statistic: identifying differences in brain networks. Neuroimage 2010; 53: 1197–207.
Zhou B, Yao H, Wang P, Zhang Z, Zhan Y, Ma J, et al. Aberrant functional connectivity architecture in Alzheimer's disease and Mild cognitive impairment: a whole-brain, data-driven analysis. Biomed Res Int 2015; 2015: 1–9.